LRP 444/91 December 1991

CROSS-FIELD DIFFUSION QUENCHING BY NEUTRAL GAS INJECTION IN A MAGNETIZED PLASMA

A. Fasoli, F. Skiff, T.N. Good, P.J. Paris

CROSS-FIELD DIFFUSION QUENCHING BY NEUTRAL GAS INJECTION IN A MAGNETIZED PLASMA

A. Fasoli, F. Skiff[a], T.N. Good[b], P.J.Paris

Centre de Recherches en Physique des Plasmas
Association Euratom - Confédération Suisse
Ecole Polytechnique Fédérale de Lausanne
21, Av. des Bains - CH-1007 Lausanne - Switzerland

Abstract

Cross-field transport of test ions is investigated in a linear Q-machine plasma. Test particles are created and followed in their motion by an optical tagging diagnostic scheme. Direct information on ion diffusivity is obtained from a comparison between the actual tag signal and a simple theoretical simulation. Diffusion is demonstrated to be supported by classical mechanisms. When different noble buffer gases are injected, the plasma reacts in such a way that the diffusivity remains classical but its magnitude is considerably reduced.

[a] Permanent address: Lab. of Plasma Research, Univ. of Maryland, College Park MD 20742, U.S.A.

[b] Present address: Department of Physics, Gettisburgh College, Gettisburgh USA.

The transport of charged particles across magnetic field lines represents one of the critical issues in characterizing the dynamical behavior of a magnetized plasma[1]. In laboratory devices, for instance, it has a strong influence over macroscopic confinement properties and consequently global machine performance. Macroscopic plasma transport is the result of the combination of a large number of individual particle displacements. Whether this constitutes a truly diffusive (irreversible) process or not depends upon the nature of correlations in the charged particle trajectories. A direct observation of the motion of a sub-set of plasma particles can prove that a description based on a diffusion equation formalism is a good approximation of the actual phenomena.

Once the diffusive character of the cross-field motion is established, the goal is to understand the kinetic mechanisms responsible for the diffusion, possibly in a quantitative way. In fact, transport processes cannot be uniquely determined by macroscopic plasma bulk observations. Special methods are required. Both the development of these methods and the basic physical questions (e.g. the kind of collisions contributing to the cross-field particle fluxes) are important for magnetic fusion research. Of particular relevance to both laboratory and space experiments is the case of partially ionized plasmas, in which neutral particles can play a critical role.

In the experiment reported herein, we investigate ion diffusion processes in a cylindrical, uniformly magnetized quiescent plasma. Our attention is focused on cross-field diffusivity and in particular on the effects of the injection of different species of non-reactive neutral gas, at different pressures. The technique of optical tagging[2,3] is used to create sets of test-ions and to follow them in their subsequent space-time evolution in order to learn about the nature of particle orbits. Even though test-particle diffusivity does not directly correspond to bulk plasma diffusion, the collisional mechanisms and parameters, once identified, can then be extrapolated and used to describe bulk transport processes[4]. This technique has been previously applied to quiescent[5] and weakly turbulent plasmas[3,6].

In our case, the plasma is demonstrated to behave classically. The injection of buffer gas is observed to reduce the value of the cross-field

diffusion coefficient. An explanation of this apparently contradictory result is proposed in terms of a modification of velocity space ion distributions caused by ion-neutral collisions.

The experiments are performed on the Linear Magnetized Plasma (LMP) Q-device[7], a uniformly magnetized (B<0.3 T) barium plasma column. For the unperturbed target plasma, temperatures are determined by the barium vapor ionizing assembly: $T_e \cong T_{\perp} \cong 2T_{\parallel} \cong 0.2$ eV; the density is in the 10^9-10^{10} cm^{-3} range. Throughout the plasma volume, barium can be considered fully ionized: resonant charge exchange is not an important loss mechanism[8]. The potential difference between the hot plate and the plasma causes a drift v_D for the ions of the order of 10^5 cm/sec. The degree of spatial and temporal fluctuation for the B field is kept below 10^{-3}. Over the central region of the plasma column (about 1.5 cm on both sides), fluctuation levels for the plasma parameters (e.g. $\delta n/n$) never exceed 5×10^{-2}; plasma azimuthal rotation is also limited ($<10^3$ rad/s). The experimental arrangement is shown in fig.1a.

Test ions are created by optical spin state tagging[9]. A first laser beam pumps one spin sub-level of the ion ground state to the first excited state via resonance absorption. Rapid decay of the excited state redistributes the pumped ions to all the ground state sub-levels. The net result of optical pumping is a depletion of the pumped sub-level and an enhancement in the state density of the unpumped sub-levels. The spin-polarized ions are then detected by observing the relative change in the fluorescence induced by a second laser beam (the "search") tuned to the same transition. The "dark signal" scheme is used: tag and search are performed on the same Zeeman line. The tagged particles will manifest themselves as a reduction in the search signal; this reduction will be called "tag signal". In our case, the two beams are issued from the same laser source (cw dye laser, P<100 mW). The laser bandwidth ($\Delta\omega \approx 1$ MHz) allows a sub-Doppler selection of the velocity class of the observed particles. The geometrical arrangement is shown in fig.1b. The tag beam is injected vertically, along a chord which can be scanned across the full diameter of the plasma cross section. The search beam is directed to the plasma at 45^0 with respect to the tag. The fluorescence is measured at the center of the plasma column. Both search beam injection and

detection apparati are mounted on a carriage[10], which can be continuously scanned along the solenoidal B-field axis.

Quantitative information, such as the value of diffusion coefficients, can be extracted from the tag signal via a comparison with a theoretical simulation. At the tag location, the ions which satisfy tag conditions become test-particles. A tag acceptance function $T(\underline{x}_0,\underline{v}_0)$ can be approximated by the expression:

$$T(\underline{x}_0,\underline{v}_0) \cong \exp\left(-\frac{(v_1 + v_{0y})^2}{\Delta\omega^2}\right) \exp\left(-\frac{(x_0 - x_T)^2}{a^2}\right) \delta(z_0 - z_T) \qquad (1)$$

where v_1 is the resonant velocity, determined by the laser frequency, a is the geometrical size of the tag beam, and x_T, z_T its cartesian coordinates. Subsequent evolution depends naturally on plasma particle dynamics; the main features, such as the presence of constants of motion, can be included in the conditioned probability function $P(\underline{x},\underline{v},t: \underline{x}_0,\underline{v}_0,t-\tau)$. P represents the probability of finding in the phase space volume $(\underline{x}+d\underline{x},\underline{v}+d\underline{v})$ at the time t a particle started at time $t-\tau$ in the volume $(\underline{x}_0+d\underline{x}_0,\underline{v}_0+d\underline{v}_0)$. The simplest approach consists of assuming that the tagged particle density n satisfies the diffusion equation:

$$\frac{\partial n}{\partial t} - D_\perp \frac{\partial^2 n}{\partial \underline{x}_\perp^2} = 0 \ , \quad \text{or} \quad \frac{\partial n}{\partial t} - D_\parallel \frac{\partial^2 n}{\partial z^2} - v_D \frac{\partial n}{\partial z} = 0 \quad (D_\perp = D_x = D_y;\ D_\parallel = D_z) \qquad (2)$$

For diffusion generated only by elastic collisions, with $v_\perp$ and $v_\parallel$ constants of motion, P can be written as:

$$P(\underline{x}, \underline{v} : \underline{x}_0, \underline{v}_0, \tau) \cong \frac{1}{v_\perp} \delta\,(v_\perp - v_{0\perp})\ \delta\,(\phi - \phi_0 + \Omega\tau)\ \delta(v_\parallel - v_{0\parallel})$$

$$\times \frac{\exp\left(-\frac{(x - x_0)^2}{4D_\perp\tau}\right)}{\sqrt{4\pi D_\perp\tau}} \frac{\exp\left(-\frac{(y - y_0)^2}{4D_\perp\tau}\right)}{\sqrt{4\pi D_\perp\tau}} \frac{\exp\left(-\frac{(z - z_0 + v_D\tau)^2}{4D_\parallel\tau}\right)}{\sqrt{4\pi D_\parallel\tau}} \qquad (3)$$

τ is the time along particle trajectories (note that t does not appear in the expression), Ω the ion cyclotron angular frequency, and ϕ the angle of the

velocity in cylindrical coordinates. P acts as a propagator on tagged particles from the tag to the search stage; the distribution of tagged particles arriving at the search beam location is:

$$f_{tp}(\underline{x},\underline{v},t) = \int_{\Re^3\otimes\Re^3} d\underline{x}_0 d\underline{v}_0 \int_{\Re^+} d\tau A(t-\tau) f_0(\underline{x}_0,\underline{v}_0) P(\underline{x},\underline{v},t : \underline{x}_0,\underline{v}_0,t-\tau) T(\underline{x}_0,\underline{v}_0) \tag{4}$$

here f_0 is the background distribution and $A(t-\tau)$ is the time dependence of the tag beam intensity (e.g. for a "chopped" laser $A=\cos[\omega_{chop}(t-\tau)]$).

To be detected, the tagged particles have still to satisfy search beam resonance conditions, expressed by the search acceptance function S:

$$S(\underline{x},\underline{v}) \cong \exp\left(-\frac{(v_1 - (v_x + v_y))^2}{\Delta\omega^2}\right) \exp\left(-\frac{x^2+y^2}{b^2}\right) \delta(z - z_S) \tag{5}$$

(b is the search beam width, z_S its axial coordinate).

Finally, the tag signal will be:

$$N(t) = \int_{\Re^3\otimes\Re^3} d\underline{x} d\underline{v} f_{tp}(\underline{x},\underline{v},t)\, S(\underline{x},\underline{v}) \tag{6}$$

Under the assumption of a maxwellian unperturbed distribution, all but the time integral can be performed analytically.

In fig.2 the z evolution of the calculated tag signal is displayed together with the actual data. Both traces show an oscillatory behavior, which is originated by the cyclotron orbit dependence of the tag signal integral. Of utmost concern, though, is the radial profile, in view of a determination of the perpendicular diffusion coefficient. In expression (6), the term which contains the radial evolution has a gaussian form, with a full width at half maximum (FWHM) given by[5]:

$$FWHM \cong \left(2.77\,(a^2 + b^2 + 4D_\perp \tau)\right)^{1/2} \tag{7}$$

Due to the uniform plasma drift, the time variable can be transformed into a spatial variable: $\tau=(z_S-z_T)/v_D$. As the tag-search distance is increased, a spreading in the tag profile should be observed. We show in fig.3, superimposed on the density profile, the measured tag profile at two different axial positions, as well as the theory simulation for one of the two cases.

A confirmation *a posteriori* of the diffusive character of the radial spreading of test particles, and a validation of the transfer function used in the simulation, can be obtained by recording the tag profile at several z-locations. In the case of diffusion, as can be seen from eq.(7), the FWHM must scale as the square root of the distance. This means in more general terms that the particles undergo a cross-field random motion ($\Delta x \propto \sqrt{t}$). In fig.4 we show that in the actual plasma this is the case. After a certain distance, though, when the particles arrive to the plasma edge, the dependence of $FWHM^2$ on tag-search separation is no longer linear; the motion is there influenced by gradients and associated local instabilities, mainly drift oscillations. Moreover, the plasma rotation, not negligible at the plasma edge, can lead to an incorrect interpretation of the tag signal evolution. In the following we will refer only to measurements performed in the flat central region of the plasma profile*.

From series of tag profile records, and independent measurements of v_D, the value of the perpendicular diffusion coefficient for different plasma conditions can be obtained. Of fundamental interest is the dependence of $D_\perp$ on the magnitude of the confining magnetic field (fig.5). We observe a B^{-2} scaling, which indicates that the diffusion is regulated by classical mechanisms. Stated otherwise, the basic step for the random motion in the cross-field direction is the particle Larmor radius (ρ_i). This agrees with theoretical predictions[4] and previous observations[5] relevant to plasmas with low intensity levels of fluctuating fields. The perpendicular diffusion coefficient is given by $D_\perp=1/2\rho_i^2\nu_{eff}$, where ν_{eff} is an effective collision frequency. The magnitude of the observed test-ion diffusion coefficient agrees with this expression when for ν_{eff} the ion-ion Coulomb collision frequency (ν_{ii}) is considered. Bohm's

*Based on experimental measurements of plasma rotation, the contribution of rotation to the width of the tag profile can be evaluated: for the cases of interest it never exceeds 10% and will therefore be neglected.

prediction[11] for anomalous diffusion would yield values larger than measured by almost a factor of two. For the observed fluctuation levels, turbulent diffusion[12], on the other hand, would be characterized by a much smaller $D_\perp$. Moreover, these two non-classical mechanisms for diffusion are independent of the plasma density; on the contrary, we do observe a linear dependence of the radial diffusion on the density, as predicted by classical theory.

When neutrals are injected, the number of possible binary collisions for the plasma ions is expected to increase. Not only ions can collide with each other via Coulomb fields, but they can also be scattered by gas atoms or molecules through different sorts of short range interactions. Starting from a classical regime, which in a sense corresponds to a "minimum diffusion" state for a given plasma configuration, perpendicular diffusivity should increase. Instead, the experimental observations indicate that, for the explored pressure regimes (which cover the operational range for the plasma Q-source), the cross-field diffusion coefficient is reduced. As shown in fig.6, the heavier the noble gas, the more important is this reduction.

In order to understand this effect of diffusion quenching by neutrals, measurements of the modified ion velocity distributions have been taken. Neutrals modify substantially, via momentum exchanging elastic collisions**, perpendicular and parallel distributions. In fig.8 the perpendicular ion temperature and the drift velocity are plotted as a function of buffer gas mass. A net reduction in both $T_\perp$ and v_D is observed, while $T_{||}$ (not shown) increases slightly for He and Ne and stays approximately constant for heavier gases. The reason for this is that the neutral "friction" force takes directly energy out of the distributions, but at the same time can partly thermalize drift ordered energy and transform it into parallel temperature. This implies that the ion-ion collision frequency, which depends upon the overall ion thermal spreading, is not much affected, and that the ion Larmor radius is substantially reduced. ρ_i tends, somehow self-consistently, to remain smaller than the mean free path for ion-neutral collisions and therefore to remain the elementary microscopic step for the cross-field particle

**A partial proof that collisions are elastic comes from the total ion energy balance, and its observed dependence on gas mass and pressure (fig.7).

transport process. So, the buffer gas atoms do not modify directly the diffusion mechanism, which is always classical (see theory points in fig.6), as confirmed by the observed inverse dependence of $D_\perp$ on the B-field intensity. The effect of ion-atom collisions is rather to enhance the coupling between the configuration and velocity space diffusivity, i.e., more formally, the significance of the off-diagonal terms of the global phase space diffusion operator.

Typical operating pressures were in the range of 10^{-6}÷10^{-4} torr. By varying the pressure, that is the ratio of the neutral to the ion density, the same kind of response is found, for different buffer species. In fact, the effects of perpendicular cooling and parallel thermalization of drift motion keep up with the observed reduction of cross-field particle fluxes: over the whole pressure range the diffusive transport is quenched even though the physical transport mechanism is kept the same. In fig.9 the case of Xenon is taken as representative of the variation of $D_\perp$ with the injection pressure. It has to be noticed that for pressures larger than a critical value, the contribution to the cross-field flux of ion-neutral (in) collisions overcomes that of ion-ion (ii) collisions. The total value of the perpendicular coefficient, then, starts to increase as a function of the neutral number density. The inversion point, for which $\nu_{in} \approx \nu_{ii}$, can be predicted theoretically; an agreement with the actual data is found if an ion-atom transport cross section derived from polarization interaction is considered ($\sigma^t \approx 10(\alpha_d e^2/E_k)^{1/2}$, where α_d is the atom polarizability and E_k the kinetic energy of the relative motion[13]).

To summarize, a direct measurement of test-ion transport across an uniform magnetic field has been performed via a non perturbative diagnostic method. Diffusion is demonstrated to be originated by classical mechanisms, even when buffer noble gases at relatively high pressures are injected in the machine. The modifications of ion velocity distributions by ion-atom collisions are such that the ion Larmor radius is reduced in the presence of the neutral gas and it remains the elementary step of the random motion which supports diffusion across the B-field. The associated macroscopic transport is then quenched. A coupling between velocity and configuration space diffusion is suggested. The limit value for the pressure, at which ion-atom collisions start to become important even in configuration space transport could be inferred for the

different cases. The experimentally observed strong dependence of test-ion diffusion on background plasma parameters confirms a possible use of the injection and detection of test particles as a sensitive probing method in different plasma environments[14,15]. Based on the possible ion velocity selectivity of this diagnostic scheme, further applications can be proposed in the field of wave-particle interaction, where resonant classes of particles can undergo important changes in their phase space diffusivity.

Acknowledgements

This work was partially supported by the Fonds National Suisse de la Recherche Scientifique. We would like to thank M.Q.Tran for comments on the manuscript, R. Kleiber for help with the experiments and K.Appert for useful discussions. One of us (F.S.) acknowledges support from the Alfred P. Sloan Research Fellowship and a NSF PYI award.

References

1 R. Balescu, *Transport Processes in Plasmas* (North Holland, Amsterdam, 1988)
2 R.A.Stern and J.A.Johnson, *Phys. Rev. Lett.*, **34**, 1548 (1975).
3 R.A.Stern, D.N.Hill and N.Rynn, *Phys. Lett.*, **93A**, 127 (1983).
4 N.Rostoker and M.N.Rosenbluth, *Phys. Fluids* **3**, 1 (1960).
5 R.McWilliams and M.Okubo, *Phys. Fluids* **30**, 2849 (1987).
6 R.McWilliams, M.Okubo and N.S.Wolf, *Phys. Fluids B* **2**, 523 (1990).
7 P.J.Paris and N.Rynn, *Rev. Sci. Instrum.* **61**, 1096 (1990).
8 E.W.McDaniel, *Collisional Phenomena in Ionized Gases* (J.Wiley & Sons, New York, 1964), Chapter 6.
9 F.Skiff et al., *Phys. Lett. A*, **137**, 57 (1989).
10 F.Anderegg et al., *Rev. Sci. Instrum.* **59**, 2306 (1988).
11 D.Bohm, in *The Characteristics of Electrical Discharges in Magnetic Fields*, edited by A.Guthrie and R.K.Wakerling (McGraw-Hill, New York, 1949) p.77.
12 T.H.Dupree, *Phys. Fluids* **10**, 1049 (1967).
13 H.S.W.Massey, *Electronic and Ionic Impact Phenomena*, Volume III (Oxford University Press, Oxford, 1971).
14 J.-H. Wang and T.C.Marshall, *Phys. Fluids B* **3**, 1687 (1991).
15A Valenzuela et al., *Nature* (London) **320**, 700 (1986).

Figure captions

Fig. 1(a) Experimental set-up. (b)Geometry for tag and search beam injection.

Fig. 2 Axial evolution of the tag signal. Δz is the tag-search separation. No diffusion effect is considered in the simulation; no gas is injected. r=0.4 cm; B≅1.5 kG; the laser frequency corresponds to $v_1/v_{\perp th}\cong 0.2$.

Fig. 3 Radial scan of the tag signal, displayed on the same scale as the density profile. Units on vertical axis are arbitrary. $v_1/v_{\perp th}\cong 0$; B≅1.5 kG; no buffer gas. Only one theory curve is shown, for clarity purposes.

Fig. 4 Square of the tag radial profile FWHM as a function of the tag-search separation; parameters are the same as for fig.3. A least square fit for $\Delta z<30$ cm is also shown.

Fig. 5 B-field scaling of the measured perpendicular diffusion coefficient (no gas). Here, as in the successive graphs, $v_1/v_{\perp th}\cong 0$, but the same behavior is observed for different velocity classes.

Fig. 6 Perpendicular diffusion coefficient vs. the mass of the injected buffer gas. $n_0\approx 10^{10}$ cm^{-3}, $p\approx 3\times 10^{-4}$ Torr, B≅1.9 kG. The open circles are calculated from $D_\perp=1/2\rho_i^2\nu_{ii}(\max[T_\perp,T_\parallel])$. For heavy gases, when $v_D<1\times 10^4$ cm/s, $D_\parallel$ can also be estimated; its order of magnitude (10^5 cm^2/s) agrees with the expected value $D_\parallel=T_i/\mu\nu$, where μ the reduced mass and ν the sum of ion-ion, ion-electron, and ion-atom collision frequencies.

Fig. 7 Total ion kinetic energy, including drift, parallel and perpendicular thermal motions, as a function of the buffer gas mass. $p\approx 3\times 10^{-4}$ Torr. The solid line corresponds to the expected losses due to ion-atom elastic collisions.

Fig. 8 Effects of buffer gas injection on plasma characteristics: $T_\perp$ (a) and v_D (b) vs. gas mass number. Same parameters as in fig.6.

Fig. 9 Variation of the measured $D_\perp$ with the buffer gas pressure, in Xenon. $n_0 \approx 10^9$ cm^{-3}; B≅1.9 kG.

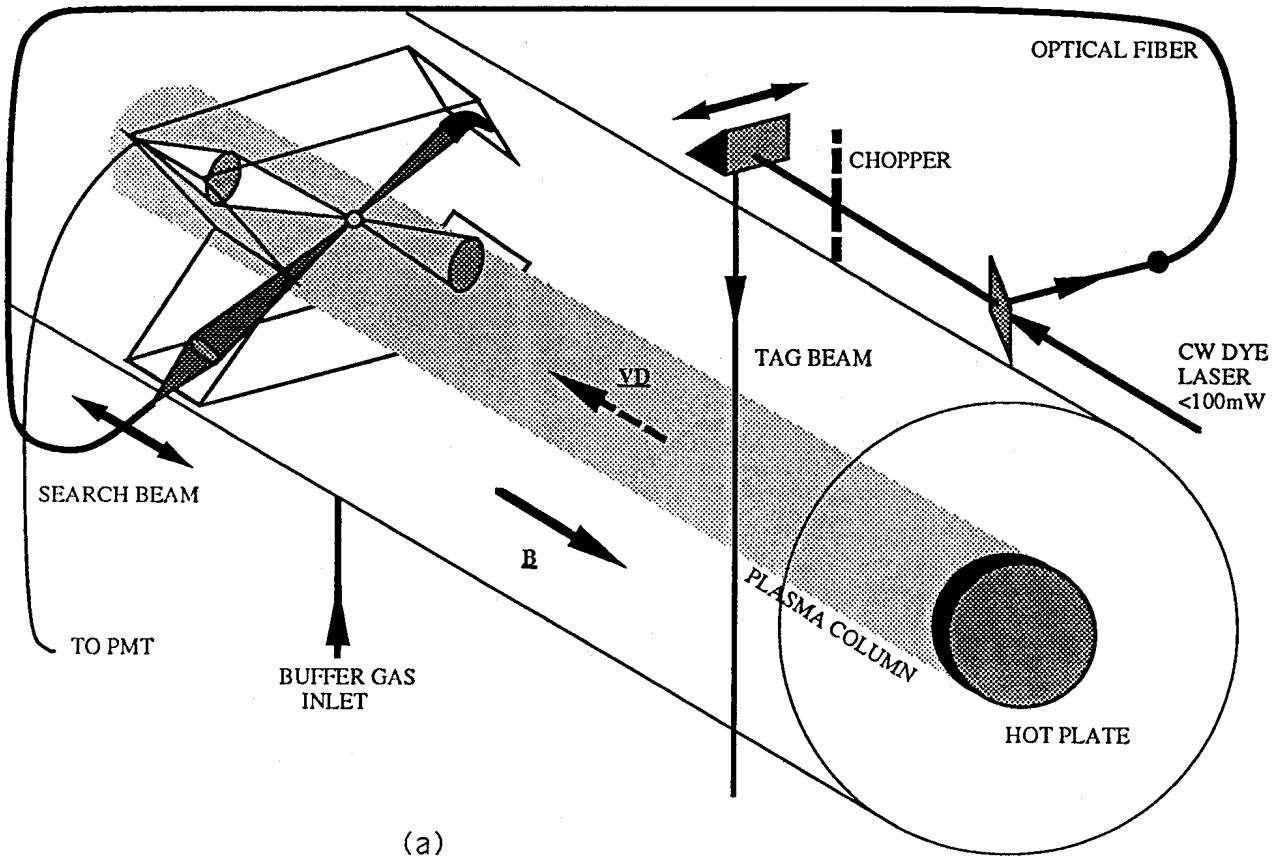
OPTICAL FIBER
CHOPPER
TAG BEAM
CW DYE
LASER
<100mW
VD
SEARCH BEAM
B
PLASMA COLUMN
TO PMT
BUFFER GAS
INLET
HOT PLATE

(a)

Fig. 1

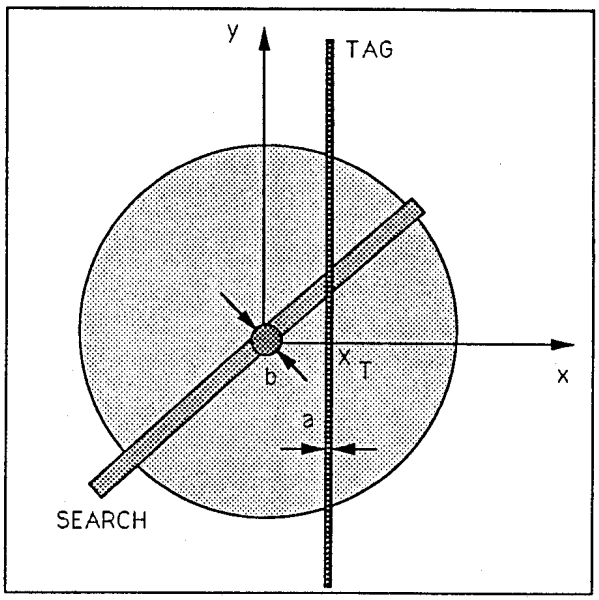
y
TAG
x
T
b
a
SEARCH

(b)

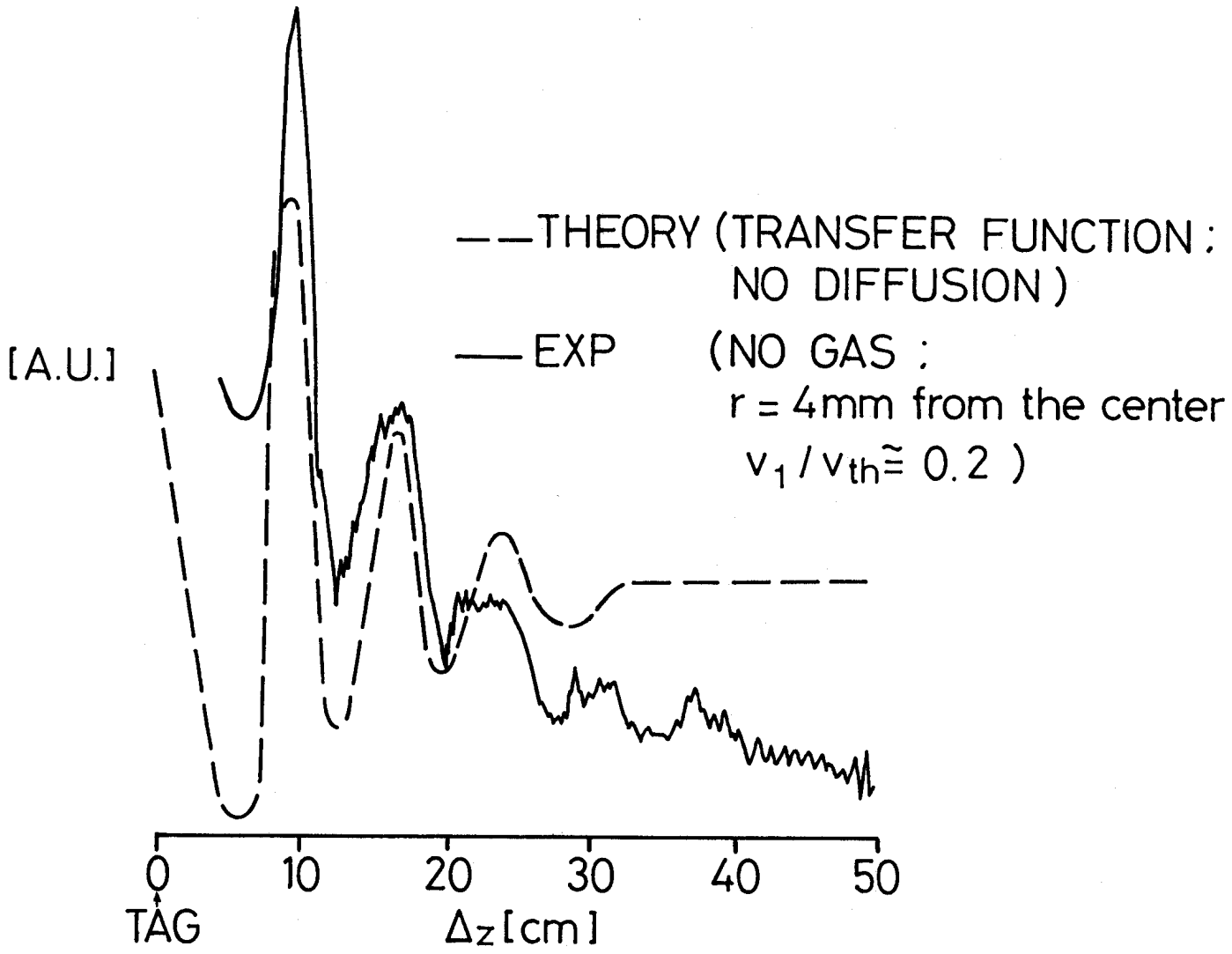
[A.U.]
——THEORY (TRANSFER FUNCTION :
NO DIFFUSION)
—— EXP (NO GAS :
r = 4mm from the center
$v_1 / v_{th} \cong 0.2$)
0
10
20
30
40
50
TAG
Δz [cm]

Fig. 2

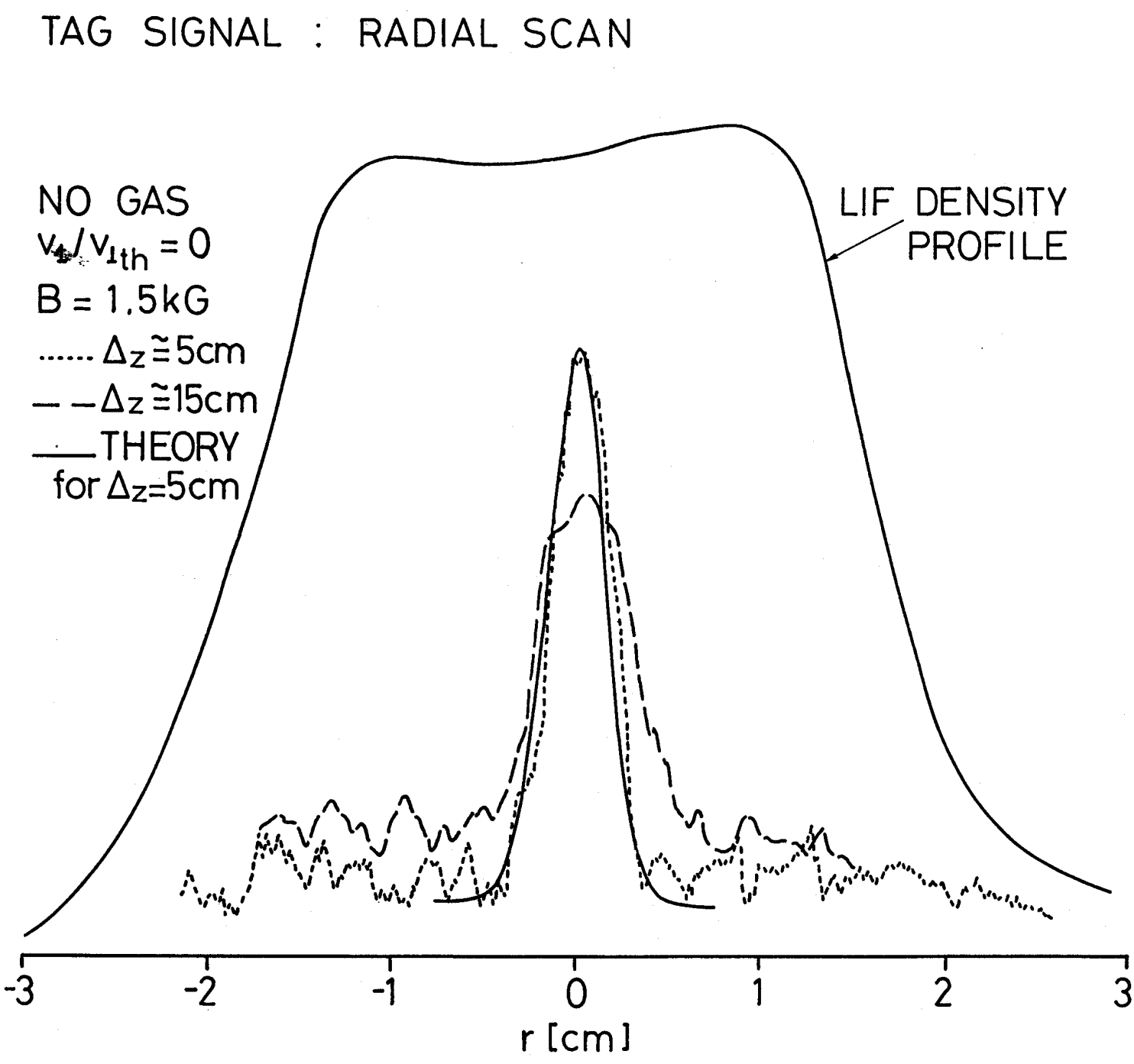
TAG SIGNAL : RADIAL SCAN
NO GAS
$v_{\perp}/v_{\perp th} = 0$
B = 1.5kG
..... $\Delta z \cong 5$cm
— — $\Delta z \cong 15$cm
—— THEORY
for $\Delta z = 5$cm
LIF DENSITY
PROFILE
-3
-2
-1
0
1
2
3
r [cm]

Fig. 3

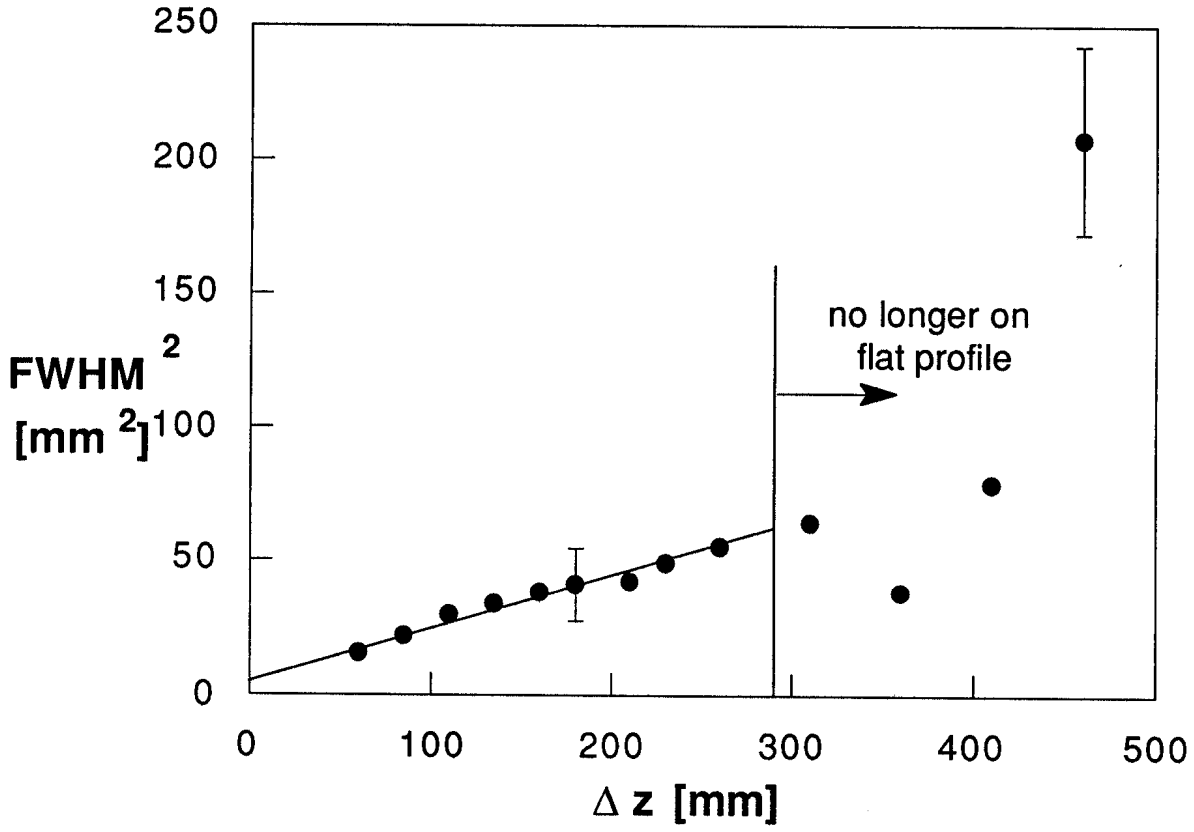
250
200
150
100
50
0
FWHM 2
[mm 2]
no longer on
flat profile
0
100
200
300
400
500
Δ z [mm]

Fig. 4

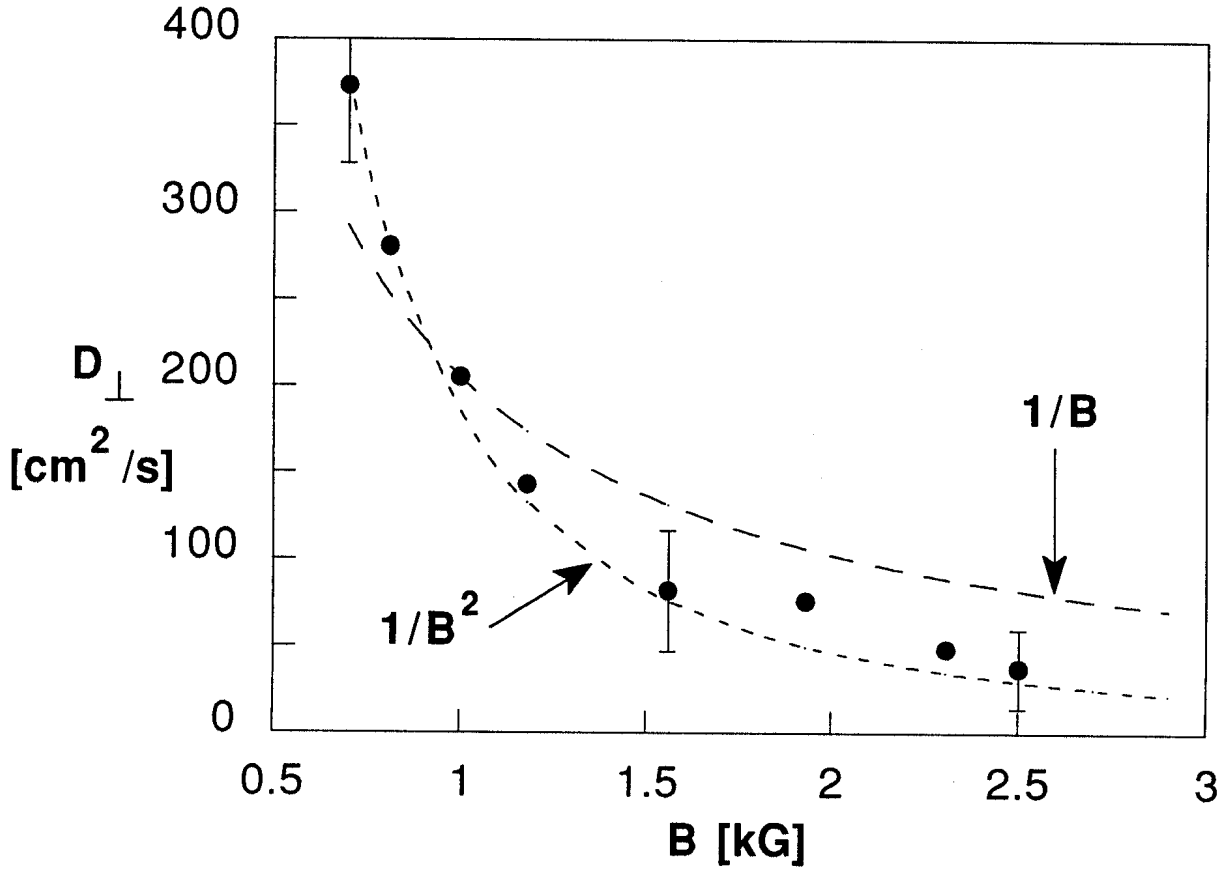
400
300
200
100
0
D⊥
[cm 2 /s]
1/B
1/B 2
0.5
1
1.5
2
2.5
3
B [kG]

Fig. 5

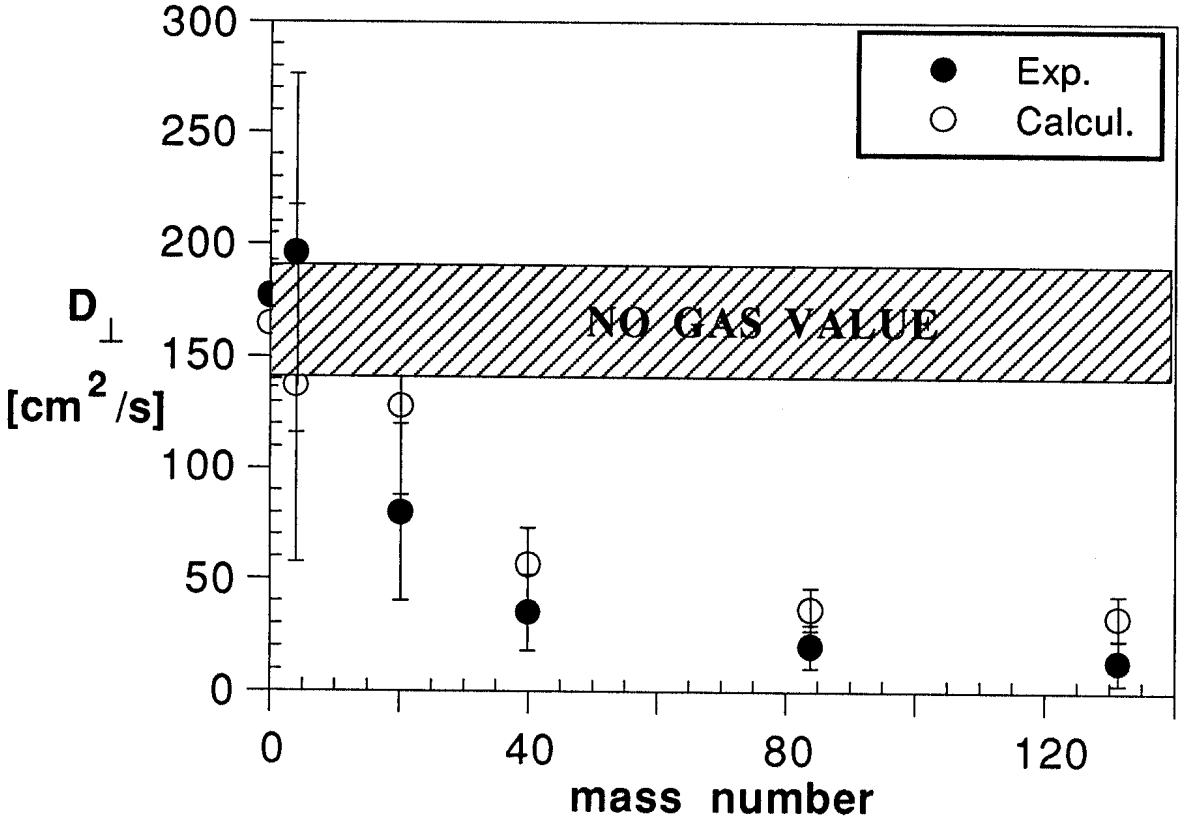
300
250
200
150
100
50
0
$D_\perp$
[cm^2/s]
Exp.
Calcul.
NO GAS VALUE
0
40
80
120
mass number

Fig. 6

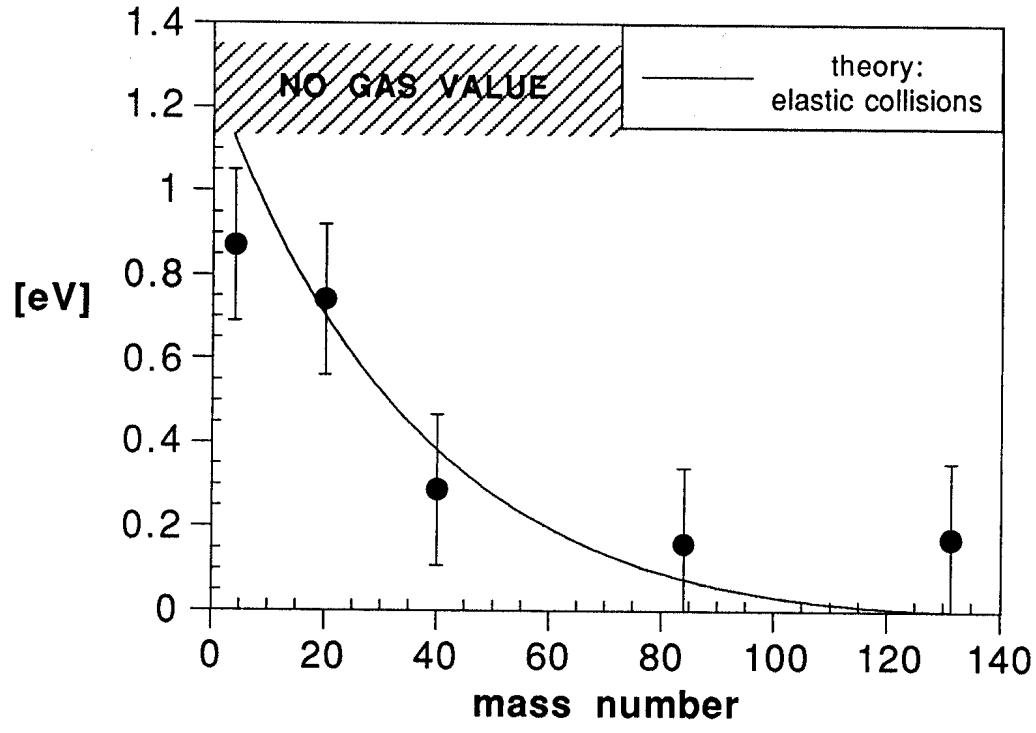
1.4
1.2
1
0.8
0.6
0.4
0.2
0
[eV]
NO GAS VALUE
theory:
elastic collisions
0
20
40
60
80
100
120
140
mass number

Fig. 7

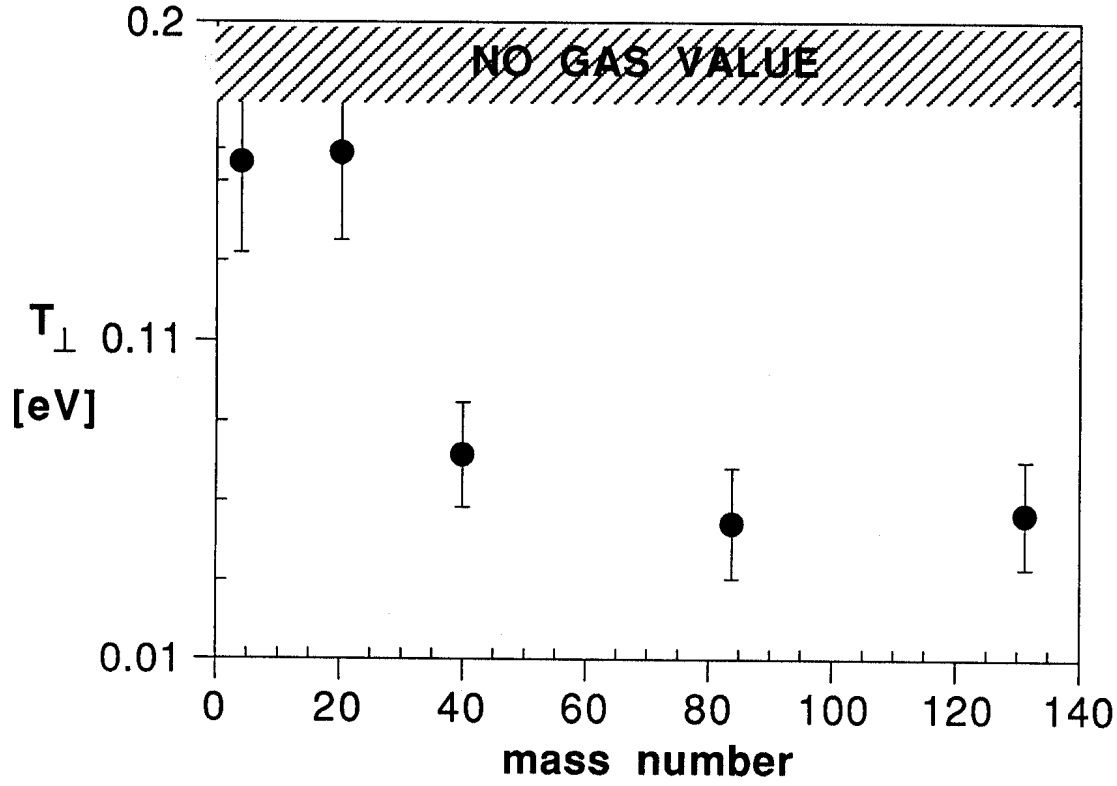
0.2
NO GAS VALUE
$T_\perp$ 0.11
[eV]
0.01
0
20
40
60
80
100
120
140
mass number

(a)

Fig. 8

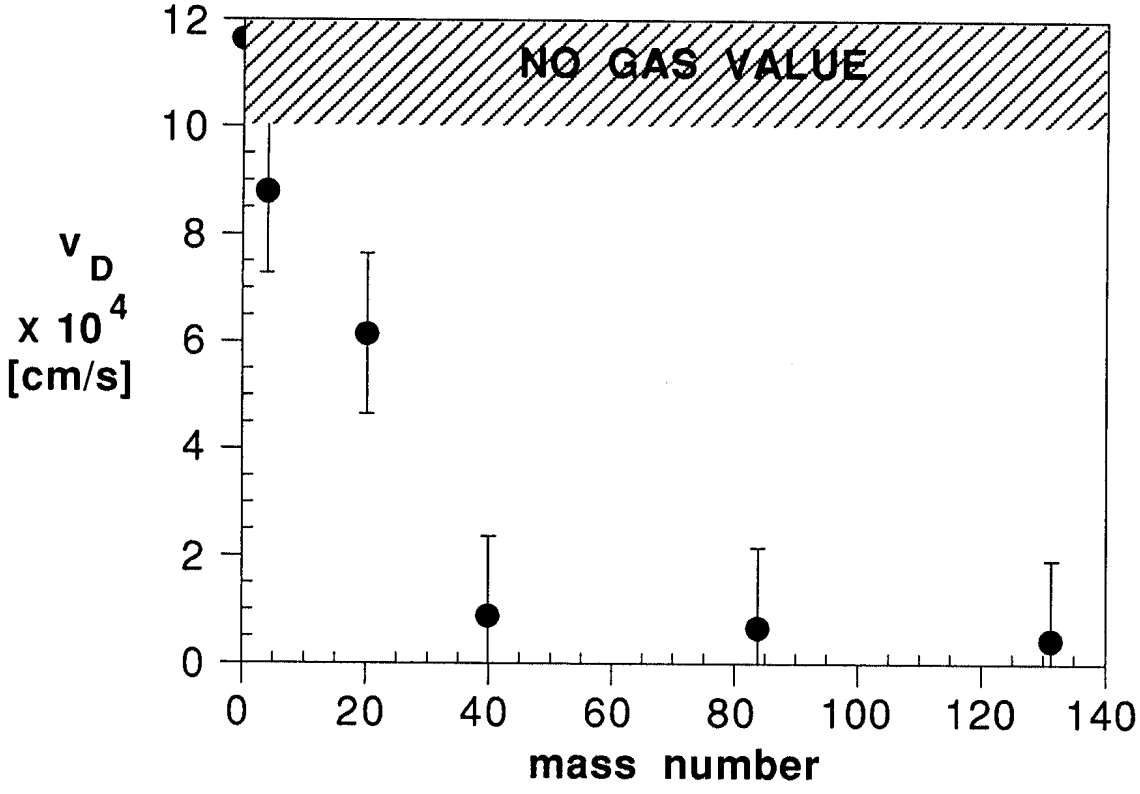
12
NO GAS VALUE
10
8
v_D
x 10^4
[cm/s]
6
4
2
0
0
20
40
60
80
100
120
140
mass number

(b)

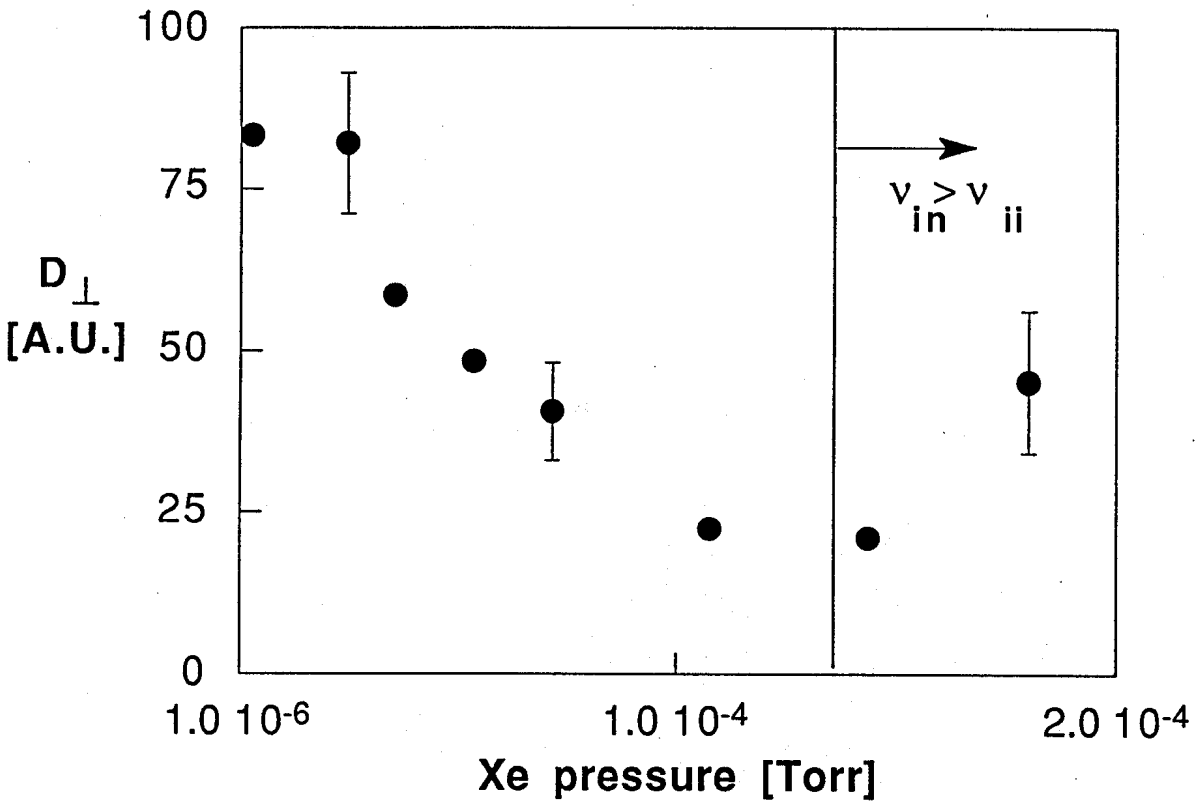

Fig. 9